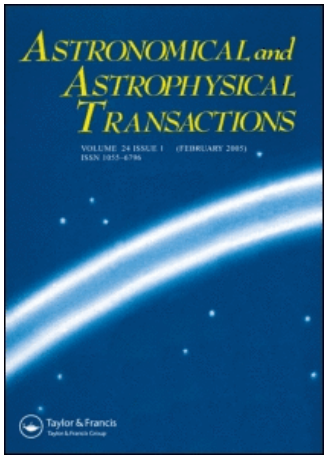

Astronomical & Astrophysical Transactions
The Journal of the Eurasian Astronomical Society
Publication details, including instructions for authors and subscription information:
http://www.informaworld.com/smpp/title~content=t713453505

On calculating the solar wind parameters from the solar magnetic field data

V. N. Obridko [a]; A. F. Kharshiladze [a]; B. D. Shelting [a]
[a]**IZMIRAN**, Russia

Online Publication Date: 01 November 1996
To cite this Article: Obridko, V. N., Kharshiladze, A. F. and Shelting, B. D. (1996) 'On calculating the solar wind parameters from the solar magnetic field data', Astronomical & Astrophysical Transactions, 11:1, 65 - 79
To link to this article: DOI: 10.1080/10556799608205456
URL: http://dx.doi.org/10.1080/10556799608205456

Astronomical and Astrophysical Transactions, 1996, Vol. 11, pp. 65–79
Reprints available directly from the publisher
Photocopying permitted by license only

ON CALCULATING THE SOLAR WIND PARAMETERS FROM THE SOLAR MAGNETIC FIELD DATA

V. N. OBRIDKO, A. F. KHARSHILADZE, and B. D. SHELTING

IZMIRAN, 142092, Troitsk, Moscow Region, Russia

(Received April 18, 1995)

It is shown that the expansion factor of the solar magnetic field is insufficient to calculate the solar wind velocity. Moreover, the magnetic field structure cannot unambiguously determine the solar wind velocity field in therms of the source surface concept and the potential magnetic field approximation in the corona. It is shown that characteristics relating the solar and near–Earth interplanetary magnetic field undergo cyclic variations.

KEY WORDS Solar wind, magnetic field, solar activity

1 INTRODUCTION

The origin of time variations of the daily mean solar wind velocity is still unknown. The classical theory of Parker (1958) gives a single universal velocity value at the Earth orbit, that is determined by the temperature in the solar corona. On the other hand, observations show the real velocity to range from 350 to 1100 km s^{-1}. These variations are partly due to solar flares and transients. However, even if these non-stationary events are ignored, the variations are still significant (350–850 km s^{-1}).

Slow variations of the solar wind (*SW*) velocity can be naturally associated with the magnetic field structure elements in the Sun, in particular, with active regions, coronal holes, large-scale field boundaries, etc. A comparison made by different authors has shown that the velocity is generally higher when the solar wind originates at open magnetic field configurations (e. g., see Obridko and Shelting, 1987; 1988). The same qualitative conclusion follows from the theory (for review see Priest, 1985). However these works do not allow a quantitative method to be developed for routine calculations of the daily mean *SW* velocity.

Wang and Sheeley (1990) introduced a new parameter – the solar magnetic field expansion at the Earth projection point, and revealed negative correlation between this parameter and the daily mean *SW* velocity for 1967–1988. This result was

theoretically interpreted in (Wang and Sheeley, 1991). The method was used in (Wang *et al.*, 1990) to calculate the latitude distribution of *SW* velocity averaged in longitude.

It should be noted, however, that Wang and Sheeley (1990) gave only a general comparison of synoptic charts of the observed and the calculated velocities. Since the measured and the calculated values display similar dependence on the solar cycle, the agreement is seemingly very good (see Figure 2 in Wang and Sheeley, 1990). However when quantitatively compared, the measured velocities averaged over 3-month intervals show poor correlation (0.57) with the values calculated from the expansion factor. No comparison of the daily means was performed by Wang and Sheeley (1990).

In this paper, we have applied a similar procedure to compare year by year the daily mean values of the measured and calculated velocities for 1978–1983. The correlation coefficient between them proved not to exceed 0.4. Moreover, it even seems at all doubtful that solar wind velocity variations be mainly determined by the field structure in the Sun.

2 COMPARISON OF THE DAILY MEAN SOLAR WINDVELOCITY AND THE MAGNETIC FIELD EXPANSION FACTOR

The expansion factor is determined in the form

$$f_s(\theta_s, \varphi_s) = \frac{R_\odot^2 B_r(R_\odot, \theta_\odot, \varphi_\odot)}{R_s^2 B_r(R_s, \theta_s, \varphi_s)} \tag{1}$$

Here, $(\theta_\odot, \varphi_\odot)$ are the photospheric coordinates of the field line that passes through the $(\theta_\odot, \varphi_s)$ point at the source surface, corresponding to the Earth projection along the field; R_s is the source surface radius; and $R_\odot$ is the radius of the Sun. In our case, $R_s = 2.5 R_\odot$.

The coordinates $(\theta_\odot, \varphi_\odot)$ are derived from (θ_s, φ_s) by intergrating the field line equation

$$\frac{\partial r}{B_r} = \frac{r \partial \theta}{B_\odot} = \frac{r \sin\theta \, \partial \varphi}{B_\varphi}. \tag{2}$$

The values of B_r, $B_\odot$, B_φ along the field line are calculated from the Hoeksema and Sherrer coefficients obtained under potential approximation.

The solar wind velocity values, V_w, obtained by Wang and Sheeley (1990) from the expansion factor, f_s, are:

$$\begin{array}{ll} V_w > 650 \text{ km/s} & f_s < 3.5 \\ 650 \text{ km/s} \geq V_w > 550 \text{ km/s} & 3.5 \leq f_s < 9.0 \\ 550 \text{ km/s} \geq V_w > 450 \text{ km/s} & 9.0 \leq f_s < 18.0 \\ 450 \text{ km/s} \geq V_w & 18.0 \leq f_s \end{array} \tag{3}$$

Table 1. The histogram of relation between the measured velocities and the velocities calculated by the method of Wang and Sheeley (1990)

(a)		*> 650.*	*650.–550.*	*550.–450.*	*< 450.0*
	> 650.	6	5	12	6
	650.–550.	14	50	78	41
	550.–450.	9	43	89	96
	< 450.	3	29	79	161
(b)		*> 650.*	*650.–550.*	*550.–450.*	*< 450.0*
	> 650.	.8	.7	1.7	.8
	650.–550.	1.9	6.9	10.8	5.7
	550.–450.	1.2	6.0	12.3	13.3
	< 450.	.4	4.0	11.0	22.3
(c)		*> 650.*	*650.–550.*	*550.–450.*	*< 450.0*
	> 650.	18.8	3.9	4.7	2.0
	650.–550.	43.8	39.4	30.2	13.5
	550.–450.	28.1	33.9	34.5	31.6
	< 450.	9.4	22.8	30.6	53.0

To give the continuous series of V_m values, this relation must be approximated as follows:

$$V_w = 380(1 + \exp(-0.093\, f_s)) \tag{4}$$

The result of (4) agrees fairly well with the original tabulated data (see Tables 1 and 2 in Obridko and Shelting, 1987).

The comparison with the measured velocity, V, was made taking into account the transport time that, unlike (Wang and Sheeley, 1990), was found by dividing the Sun–Earth distance by the measured velocity. Note that Wang and Sheeley (1990) considered the transport time constant, equal to 5 days. Our calculations carried out with the transport time both constant, and changing as a function of the actual measured velocity, have shown that correlation coefficient depends little on the transport time hypothesis with an accuracy to the 2nd decimal place.

The highest correlation between the calculated, V_m, and the measured, V, velocities is observed at the descending branch of cycle 21 (1982–1983) and is 0.375, the total number of days being 721.

However, the correlation coefficient in itself is not very equal to representative. In fact, the days of low-speed solar wind are much more frequent than the days of high-speed solar wind. It is necessary that the later situations be as reliably identified as the former. For this purpose, we have developed a matrix presented in Table 1. The Table 1 gives 3 versions of the matrix:

(a) The number of days when the observed (columns i) and the calculated (rows j) velocities fall within the given range in accordance with (3). This matrix is called n_{ij}.

Table 2. Histogram of relation between the measured velocities and those calculated from Figure 3

(a)	*> 650.*	*650.–550.*	*550.–450.*	*< 450.0*
> 650.	6	4	21	8
650.–550.	13	50	60	42
550.–450.	10	44	99	91
< 450.	3	30	78	162
(b)	*> 650.*	*650.–550.*	*550.–450.*	*< 450.0*
> 650.	.8	.6	2.9	1.1
650.–550.	1.8	6.9	8.3	5.8
550.–450.	1.4	6.1	13.7	12.6
< 450.	.4	4.2	10.8	22.5
(c)	*> 650.*	*650.–550.*	*550.–450.*	*< 450.0*
> 650.	18.8	3.1	8.1	2.6
650.–550.	40.6	39.1	23.3	13.9
550.–450.	31.3	34.4	38.4	30.0
< 450.	9.4	23.4	30.2	53.5

(b) The percentage ratio of the number of days in a given cell to the total number of records (721).

(c) The ratio of the number of days in a given cell to the total number of days when velocity was observed in the given interval ("percentage over the column").

In the ideal case of completely reliable identification, one would obviously observe concentration to the main diagonal in the matrices, and the sum of numbers in case 1b must considerably exceed 50%. As seen from Table 1, in spite of some concentration effect observed, the sum of numbers along the main diagonal in Table 1*b* is as small as 42.3%.

Another requirement is that all numbers along the main diagonal of (c) were larger than 50%, thus accounting for the difference in the occurrence of high and low velocities. Unfortunately, this requirement is not satisfied either. Only in the range of very low velocities, the reliability of indetification is 53%.

3 THE USE OF TWO-DIMENSIONAL DIAGRAMS

Thus, the situation when the velocity arises in a given range in the Sun cannot be reliable identified, proceeding from the magnetic field expansion, f_s. The expansion factor is probably the wrong parameter to choose, because the initial energy flux from the photosphere is assumed to be the same everywhere (Wang and Sheeley, 1991). In fact, there are additional heating sources in active regions, i.e. in the

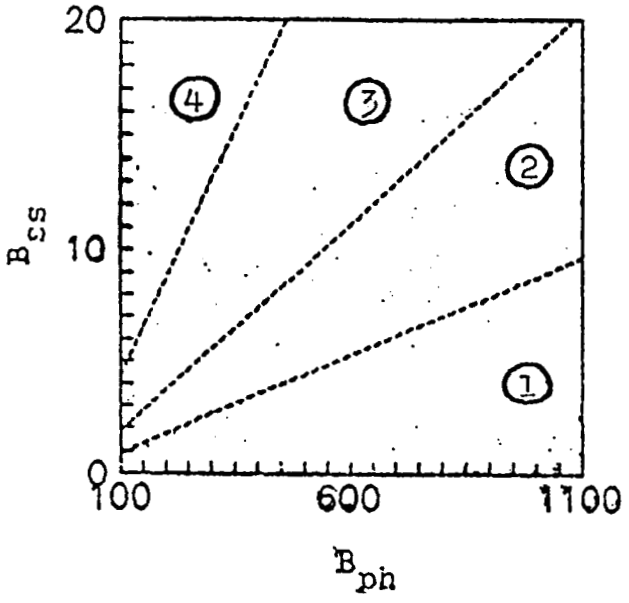

Figure 1 Velocity distribution diagram following the criterion of Wanf and Sheeley (see Eq. (3)). Region 1 corresponds to $f_s \geq 18$, ($V \leq 450$ km/s); region 2, to $9 \leq f_s < 18$ (450–550 km/s); region 3, to $3.5 \leq f_s < 9$ (550–650 km/s); and region 4, to $f_s < 3.5$ (> 650 km/s).

regions of strong photospheric fields. In this case, the dependence on magnetic fields, $B_r(R_\odot, \theta_\odot, \varphi_\odot) \equiv B_{\rm ph}$ and $B_r(B_s, \theta_s, \varphi_s) \equiv B_{\rm ss}$, is much more complicated.

The question arises whether the solar wind velocity can be unambiguously determined by two parameters, $B_{\rm ph}$ and $B_{\rm ss}$ at all. To answer this question, let us plot two-dimensional diagrams and mark on them the recorded velocities in that or another range depending on $B_{\rm ph}$ and $B_{\rm ss}$. The points on the diagrams, arranged in whatever complicated way, will form isolated clusters. Then, in the case of unambiguous relation, of $B_{\rm ph}$ and $B_{\rm ss}$ to the solar wind velocity, these clusters should not overlap. Figure 1 shows a diagram to illustrate the Wang–Sheeley condition (see Eq. (3)). Cluster 1 in Figure 1 corresponds to $f_s \geq 18$, i.e. to the velocities of ≤ 450 km/s; cluster 2 corresponds to $9 \leq f_s < 18$, i.e. to the velocities of 450–550 km/s; cluster 3 corresponds to $3.5 \leq f_s < 9$ (550–650 km/s); and cluster 4, to $f_s < 3.5$ (> 650 km/s). The field intensity in Figure 1 and further on is given in μT.

The characteristic feature of the diagram based on (3) is that all sepaation lines are the rays that emanate from the reference frame origin. In the case of enhanced velocity generation in large photosperic fields the separation lines bend and have a maximum in the regions of moderate field intensity.

In Figure 2*a*, the situations corresponding to the measured velocities $V \leq 450$ km/s are illustrated and a straight line $B_{\rm ss} = (R_\odot^2/18 \cdot R_s^2) \cdot B_{\rm ph}$ is drawn. According to the Wang–Sheeley criterion, all points must be situated below this

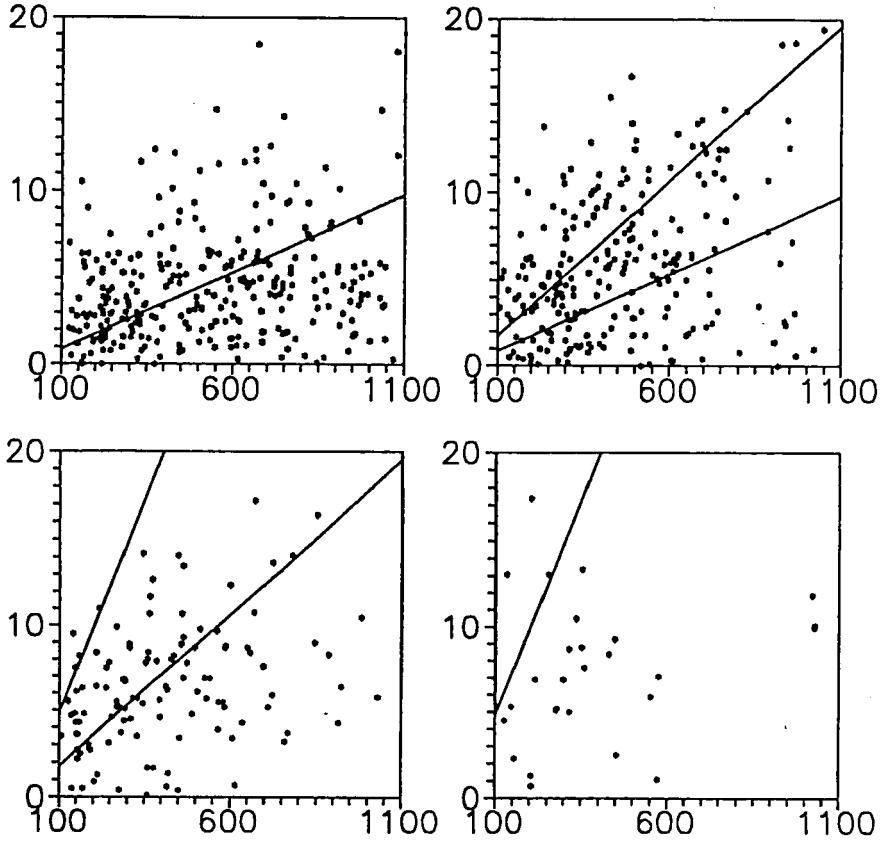

Figure 2 Distribution of measured solar wind velocities: (a), $V \leq 450$ km/s; (b), $450 < V \leq 550$ km/s; (c), $550 < V \leq 650$ km/s; (d), $V > 650$ km/s.

line. Figure 2*b* represents the points of $450 < V \leq 550$ km/s and the straight lines corresponding to $f_s = 18$ and $f_s = 9$. All points must obviously appear between the two lines. Figure 2*c* and 2*d* illustrate the points of $550 < V \leq 650$ km/s and $V > 650$ km/s, respectively, as well as the straight lines for $f_s = 9$ and $f_s = 3.5$.

As seen from Figure 2, the points spread beyond the Wang–Sheeley lines, which is another evidence of invalidity of criterion (3). A more general result is inferred from Figure 2: the solar wind velocity cannot be unambiguously determined by two parameters (the field intensities in the photosphere and at the source surface), because the clusters of points in the four diagrams overlap. No cases of isolated clusters corresponding to a given *SW* velocity range are revealed in the (B_{ph}, B_{ss}) diagram.

This means that there is no use trying to break down the (B_{ph}, B_{ss}) plane in a more reasonable way than that suggested by Wang and Sheeley. Nevertheless, we have made such an attempt by introducing a kink in the separation curves around

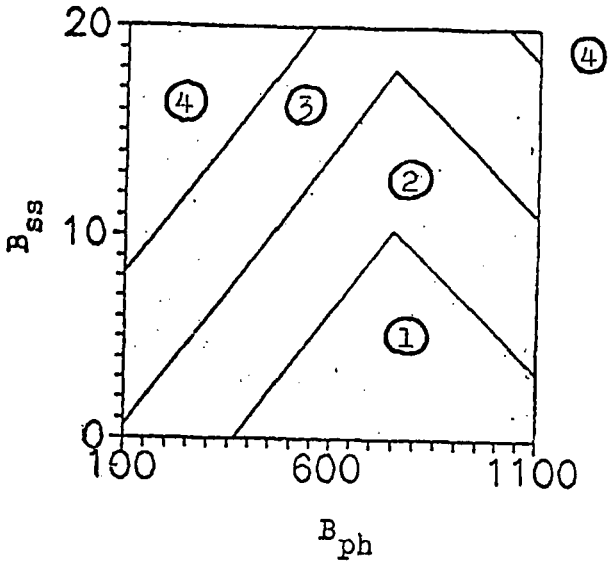

Figure 3 Velocity distribution taking into account probable heating enhancement in active regions. Conventions are the same as in Figure 1.

$B_{ph} \cong 750\mu$T. The result is shown in Figure 3. Table 2 presents the matrices correspoding to this breakdown. One can readily see that matrices in Table 1 and 2 do not differ much.

4 DEPENDENCE ON THE PHASE OF THE CYCLE

In this Section we shall consider cyclic behaviour of the solar wind velocity near the Earth depending on the solar magnetic field at the Earth projection point. We have analyzed three two-year data files chosen from the most interesting intervals of solar activity: 1989–1990 (sunspot maximum, the number of days when reliable solar wind velocity data are available $N = 719$); 1982–1983 (beginning of the descending branch, $N = 721$); and 1985–1986 (sunspot minimum, $N = 476$). The data are taken from the histograms obtained in the same way as Tables 1 and 2. The results are presented in Table 3.

Here, n_{im} is the elemet of the 4 × 4 correlation matrix, in which the largest value is achieved in every column, i. Remember that the columns correspond to the grades of measured velocities, and the rows, to the grades of calculated velocities (see Section 2 above). The % sign denotes the same elements expressed as a percentage fraction of the total number of observation days, N.

The best linear relation between the measured velocities and those calculated by the Wang–Sheeley method should, obviously, result in diagonal arrangement of the maximum elements (the n_{11}, n_{22}, n_{33}, n_{44} sequence), and the sum of %% in them

Table 3. Cyclic variation of characteristics of the matrices for the magnetic field and solar wind velocity expansion

		(a) Total field, B_r									
		1989–1990			*1982–1983*				*1985–1986*		
Without correction	n	n_{23}	n_{33}	n_{44}	n_{12}	n_{22}	n_{33}	n_{44}	n_{12}	n_{22}	n_{33}	n_{44}
	%	2	9	50	2	6	13	23	4	6	8	34
With correction	n_{ii}	n_{23}	n_{33}	n_{44}	n_{12}	n_{22}	n_{33}	n_{44}	n_{14}	n_{24}	n_{34}	n_{44}
	%	2	17	50	2	6	13	23	4	5	10	40
		(b) Global field, B_r									
Without correction	n_{im}	n_{22}	n_{32}	n_{43}	n_{12}	n_{22}	n_{32}	n_{44}	n_{12}	n_{22}	n_{32}	n_{44}
	%	3	10	25	2	9	15	16	2	5	11	19
With correction	n_{im}	n_{23}	n_{33}	n_{44}	n_{12}	n_{22}	n_{33}	n_{44}	n_{14}	n_{24}	n_{34}	n_{44}
	%	3	10	25	2	9	14	17	7	6	10	32
		(c) Measured longitudinal field, B_ρ									
	n_{im}				n_{12}	n_{22}	n_{33}	n_{44}				
	%				2	6	10	18				

should be close to 100. Unfortunately, the situation is from ideal. Let us consider the results in more detail.

Table 3 consists of 3 parts. For the first part, the magnetic field was calculated from the harmonic coefficients with l=10 (the maximum value, call it "total field"), for the second one, $l = 4$ ("global field"); while the third part is the "measured" field. Calculations for the first and the second parts were done both with the so called polar correction and without it (see Hoeksema and Sherrer, 1986).

For the "total field" without correction, the best correlation between the measured and the calculated velocities takes place at the decay and at the minimum of solar activity, though the concentration towards the principal diagonal is not too large (41–59%). At the phase of maximum, equation (4) does not work: the calculated velocities do not exceed 550 km/s. The apparent of the sum of diagonal elements is due to the growing number of days with very low activity.

By introducing polar correction we do not improve correlation at the decay and at the maximum of the cycle, and destroy it altogether at the minimum. It is explicable, because the photospheric base of the field line originating at the Earth projection point lies in the polar zone, where correction does not change magnetic field in the phase of maximum, slightly increases it in the decay phase, and nearly doubles it at the minimum of the cycle. This results in a fictious growth of the expansion factor and, thus, in a decrease of the calculated *SW* velocity, which is especially pronounced at the sunspot minimum. (All calculated velocities do not exceed 450 km/s).

To estimate contribution of the largest characteristic scales, we have applied filtration to eliminate all harmonics except $l \leq 4$. Then, according to (4), only the largest-scale elements with low magnetic field are involved in calculation of the expansion factor and *SW* velocity. This is expected to result in the decrease of the former and increase of the latter. This conclusion is corroborated by the results presented in Table 3*b* for "Global field". The matrix elements with the highest rate of coincidence of the observed and calculated velocities moved upward towards higher calculated values, yet the coincidence remained poor.

The attempt of nonlinear break-down of the (B_{ph}, B_{ss}) plane in order to take into account probable variations in the character of relation at $B_{ph} = 750$ μT (see Figure 3) failed to improve correlation between the measured and calculated *SW* velocities (like in Section 3 above), and therefore we did not include these results in Table 3.

5 ESTIMATION OF THE LOCAL FIELD EFFECT

We have used in our analysis the harmonic expansion coefficients of the magnetic field tabulated by Hoeksema and Sherrer (1986). These coefficients were calculated from the longitudinal magnetic field synoptic charts obtained at the John Wilcox Observatory, Stanford University. The calculations were performed in potential approximation under the assumption of a source surface existing at $2.5\,R_{\odot}$. This procedure allows the magnetic field to be calculated at any point of the spherical layer between the photosphere and the source surface. After the Earth projection point at the source surface is identified and the magnetic field at this point is calculated, integration of the field line equation yieds the corresponding point in the photosphere, the field components along the force line being determined by the harmonic coefficients. The last step is to determine the radial magnetic field in the photosphere at the base of the field line intersecting the Earth projection. This is the field value involved in the expansion factor estimates.

When put into practice, this simple and clear calculation scheme encounters certain difficulties. All calculations are performed taking into account only 10 harmonics ($l \leq 9$, $m \leq 9$). This is certainly enough for summation to give the source surface fields, however this is not the case when the photospheric fields are concerned. While comparing the calculated and the observed longitudinal magnetic fields in the photosphere, one can readily see that the former are underestimated, which implies that the first 10 harmonics are insufficient to calculate the magnetic field by using the spherical expansion method. Figure 4 illustrates the relation between the observed and the calculated longitudunal magnetic fields in the photosphere. Beginning with 300 μT, the calculated values are seen to be systematically lower than observations. Calculated fields stronger than 900 μT are absent at all. This implies that local fields corresponding the higher-order harmonics are systematically underestimated. Such a method, obviously, fails to provide correct expansion factor, at least during relatively high solar activity.

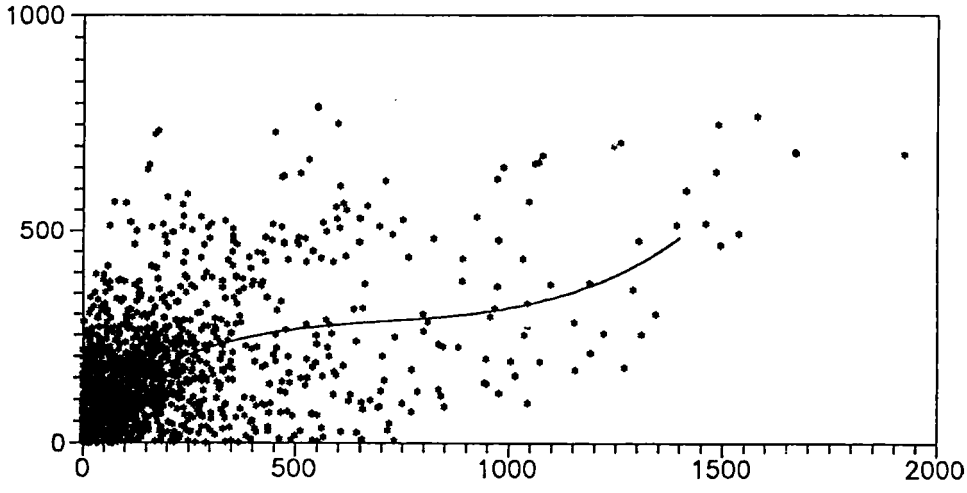

Figure 4 Relation between the observed (abscissa) and the calculated (ordinate) longitudinal magnetic fields in the photosphere.

The contribution of local fields can be estimated by using (even if not quite reasonably) the following procedure. We were unable to trace the field line experimentally. Therefore, we substituted the measured longitudinal field, $B_p(R_\odot, \theta_\odot, \varphi_\odot)$, for the calculated radial field $B_r(R_\odot, \theta_\odot, \varphi_\odot)$ in (1), and then in (4). In this case, the base of the field line was not quite correctly identified, and the expansion factor was calculated with an error. However instead we hoped to be able to estimate the contribution of local fields.

The results are shown in Table 3*b* for the descending branch of the solar cycle. One can see that the correlation of velocities did not improve by substituting the observed longitudinal field for the calculated radial field.

6 ESTIMATION OF RELIABILITY OF THE OBSERVED RELATIONS

To estimate the reliability of the relation between the observed and the calculated *SW* velocities, the selected mean square correlation of the characteristics (Korn and Korn, 1968) has been derived from:

$$f^2 = \sum_{i=1}^{4} \sum_{j=1}^{4} \frac{n_{ij}^2}{n_i \cdot n_j} - 1, \tag{5}$$

where n_{ij} are defined above, and $n_i = \sum_{j=1}^{4} n_j$, $n_j = \sum_{i=1}^{4} n_i$.

Table 4 presents the selected mean square correlation, f^2, the total number of the data pairs, N, and the quantile values, χ^2. As follows from the χ^2 distribution table, the given degree of relation has a confidence limit $cl > 99.9$ %.

Table 4.

		f^2	N	$\chi^2 = Nf^2$
1979–1980	(B_r)	0.0676	719	48.604
1982–1983	(B_ρ)	0.0838	730	61.174
1982–1983	(B_r)	0.1508	730	110.084
1985–1986	(B_r)	0.1841	476	87.632

High statistical reliability at a low correlation coefficient indicates that *SW* velocities are related to the field intensity at the ends of the field line. This relation, however, is not unambiguous, and there are other, more significant factors that determine the actual daily mean velocities.

7 DISCUSSION OF RESULTS

The conclusion that *SW* velocities cannot be unambiguously determined by the B_{ss} and B_{ph} fields is extremely important, because these are the two basic parameters that characterize solar activity. All assumptions made in the analysis are listed below.

(1) The original magnetic field data, used to calculate the expansion coefficients according to (Korn and Korn, 1968), were obtained at a spatial resolution of 3′. The velocity field fine structure under discussion can be due to small-scale features in the photospheric fields. Note, however, that trial estimates performed in Section 5 do not significantly improve correlation.

(2) The synoptic charts used in the analysis result from a synthesis of non-simultaneous observations.

(3) In our analysis, we make use of longitudinal magnetic field observations in the photosphere. All other photospheric and coronal features are calculated in potential approximation.

(4) The whole calculation procedure is based on the source surface concept. However alternative models are available, and they also should be involved in the analysis (Veselovsky, 1989).

(5) There is a probability that the velocity field fine structure arises beyond the corona, at a distance of several solar radii. Some evidence for it is presented in (Lotova *et al.*, 1985; Lotova, 1988).

8 CYCLIC VARIATIONS IN THE SOLAR WIND/GLOBAL MAGNETIC FIELD COUPLING

With direct or indirect data on photospheric magnetic fields available for a long time interval, we can analyze cyclic variations in the coupling of the stationary solar wind

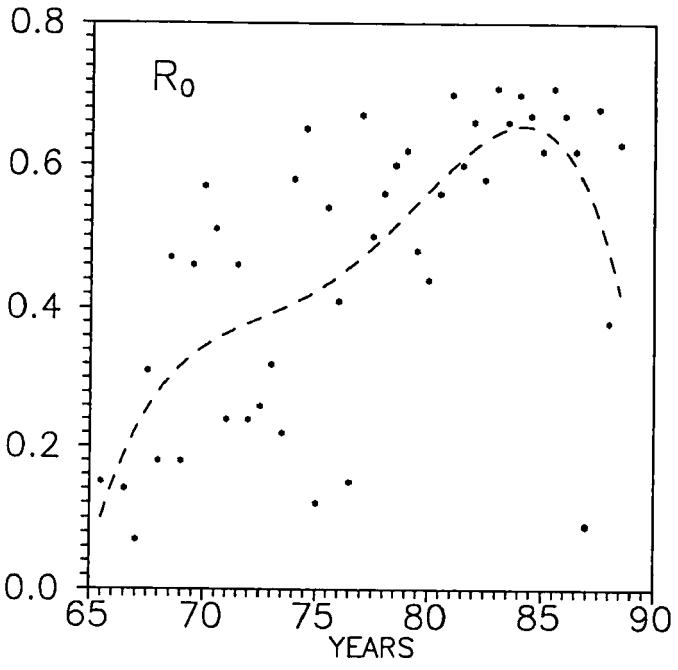

Figure 5 Correlation coefficient of the source surface field B_{ss}/r^2 and the magnetic field B_x component at the Earth orbit as a function of time.

with the calculated magnetic field on the source surface. The simplest theoretical consideration is as follows. The field beyond the source surface is mechanically transported by the solar wind and falls back proportionally to the square distance from the Sun. Therefore, the field structure observed in the Earth neighbourhood must be totally determined by the source surface field, i.e. $B_x \approx B_y$, $B_z \approx 0$, and the proportionallity coefficient for B_x and the source surface field, B_{ss}, must be close to $(R_{ss}/R_E)^2$, where R_E is the average Sun–Earth distance. Thus, the field at the Earth orbit can be derived from the source surface field by simple multiplication by scale factor $\sim 1.37 \times 10^{-4}$. Of course, the solar wind transport time from the Sun to the Earth must be taken into account. It is either a priori assumed equal to 4 or 5 days, or it is calculated by dividing the Sun–Earth distance by the solar wind velocity measured at the Earth orbit on a particular day.

This simple scheme was checked only qualitatively. It was shown that, the transport time being properly selected, 70–80% of the daily mean B_x values coincided *in sign* with B_{ss} (see for example Hoeksema and Scherrer, 1986). No systematic quantitative comparison of the values calculated following the mentioned scheme and the direct measurements was made over a long time interval.

We have carried out such a comparison over the time interval of 1965–1988. The main difficulty in studying cyclic variations of global magnetic fields and the heliosphere is due to the absence of sufficiently long data series. We have at our

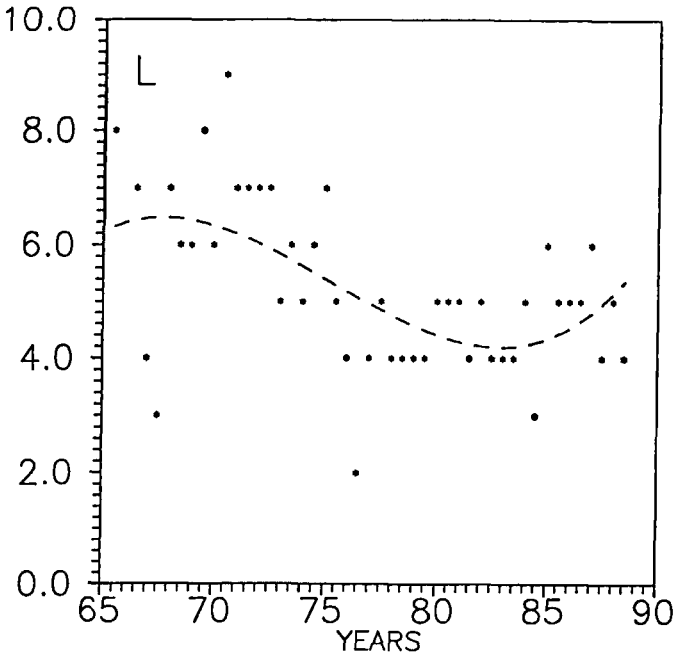

Figure 6 Shift of the correlation coefficient of the source surface field and the magnetic field B_x component at the Earth orbit as a function of time.

disposal synoptic maps of photospheric magnetic fields for the time interval from August 1959 to December 1978 (Carrington rotations 1417–1648) obtained by the group of robert Howard at the Mount–Wilson Observatory (MWO). Another series observations for Janyary 1975 – July 1984 (Carrington rotations 1622–1751) was performed under the guidance of J. W. Harvey at the Kitt–Peak Observatory (KPO). And finally, the third series of data was obtained at the Wilcox Solar Observatory of the Stanford University (WSO) and was made available to us by J. T. Hoeksema. These observations started in May 1976 (Carrington rotation 1641) and are still continued. If the photospheric magnetic field is known, then, using potential approximation and the source surface hypothesis, one can calculate the source surface field, i. e. the field at the origin of the heliosphere (e. g. see Hoeksema and Sherrer, 1986). In our analysis, we have used all three data series in spite of their nonuniformity. The data were reduced to a single scale by comparing the overlapping time intervals. As a result, the data on global magnetic fields and on three-dimentional structure of the heliosphere are now available for the past 35 years (more reliable for the past 29 years). We can also use the information on the Interplanetary Magnetic Field data (IMF data) based on the direct measurements near the Earth for approximately the same time interval.

The behaviour of the correlation coefficient of B_{ss}/r^2 with B_x, $R_0(t)$, is illustrated in Figure 5. One can readily see that during the first 10 years, the correlation

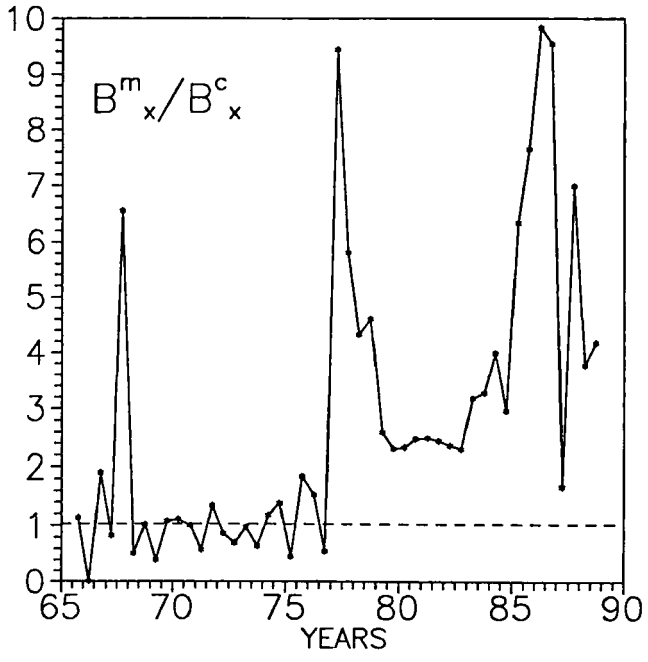

Figure 7 Ratio of the measured and the calculated magnetic field B_X components in the solar wind at the Earth orbit as a function of time.

was rather low. Then, it increased gradually, and by the middle of the 80-ies it reached 60–70%. It is not quite clear, whether we deal with a real physical change of correlating values, or whether the effect is due to nonuniformity of our data series. Anyway, we can be sure that since 1976 the data are quite uniform, and therefore Figure 5 positively displays a cyclic variation in the relation between the fields near the Earth and at the source surface.

Figure 6 illustrates the transport time defined as the time shift relative to the main maximum of the cross-correlation function, R_0 (B_{ss}/r^2, B_x). We believe it to be the parameter that best characterizes variations of the mean mass velocity with the phase of the solar cycle. The shift is seen to be maximum in the middle of the 60-ies (minimum of the solar cycle). Then, it decreased gradually to reach its minimum value by the middle of the 80-ies. Only time will show, whether the present-day growth of the shift is a real tendency, and whether we do observe a certain cyclic variation. After 1976 the cyclic variation is practically absent.

And finally, Figure 7 shows the relation between the field at the Earth orbit calculated from the scheme described above and the direct measurements. Here, two remarkable effects draw our attention. First, in the growth phase of all three cycles under consideration (20, 21, and 22), the measured fields are by an order higher that the calculated ones. At other times, the difference does not exceed the factor 2.5. Second, one readily see that the data before and after 1976 are not a

like. Before 1976, the calculated and the measured values agree amazingly well. After 1976, the measured values are at least twice as large as the calculated ones. It looks as if the MWO data used before 1976 were systematically different from the WSO data used after 1976.

References

Hoeksema, J. T. and Scherrer, P. H. (1986) *Solar Magnetic Field-1976 trough 1985, Report UAG-94*, WDCA, Boulder.

Korn, G. and Korn, T. (1968) *Refernce book on mathematics for scientists and engineers*, Nauka, Fizmatgiz, p. 569.

Lotova, N. A. (1988) *Solar Phys* **117**, 399.

Lotova, N. A., Blums, D. F., and Vladimirsky, K. V. (1985) *Astron. and Astrophys* **150**, No. 2, 266.

Obridko, V. N. and Shelting, B. D. (1987) *Geomagnetism and Aeronom* **27**, No. 2, 197.

Obridko, V. N. and Shelting, B. D. (1988) *Kinematics and Phusics of Celestial Bodies* **4**, No. 4, 29.

Parker, E. N. (1958) *Astrophys. J.* **128**, 664.

Priest, E. R. (1985) *Solar Magnetohydrodynamics*, Moscow, Mir.

Veselovsky, I. S. (1989) *Solar magnetic fields and corona*, Novosibirsk, Nauka, p. 161.

Wang, Y. M. and Sheeley, N. R. (1990) *Astrophys. J.* **355**, 726.

Wang, Y. M. and Sheeley, N. R. (1991) *Astrophys. J.* **372**, L. 45.

Wang, Y. M., Sheeley, N. R., and Nash, A. G. (1990) *Nature* **347**, No. 6292, 439.